NUMERICAL STUDY OF COEXISTING ATTRACTORS FOR THE HÉNON MAP

ZBIGNIEW GALIAS

Department of Electrical Engineering, AGH University of Science and Technology,
Mickiewicza 30, 30–059 Kraków, Poland
galias@agh.edu.pl

WARWICK TUCKER

Department of Mathematics, Uppsala University,
Box 480, 751 06 Uppsala, Sweden
warwick@math.uu.se

The question of coexisting attractors for the Hénon map is studied numerically by performing an exhaustive search in the parameter space. As a result, several parameter values for which more than two attractors coexist are found. Using tools from interval analysis, we show rigorously that the attractors exist. In the case of periodic orbits we verify that they are stable, and thus proper sinks. Regions of existence in parameter space of the found sinks are located using a continuation method; the basins of attraction are found numerically.

Keywords: Hénon map, periodic orbit, coexisting attractors, interval arithmetic

1. Introduction

The Hénon map [Hénon, 1976] $h_{a,b} \colon \mathbb{R}^2 \mapsto \mathbb{R}^2$ is an invertible map defined by:

$$h_{a,b}(x, y) = (1 + y - ax^2, bx), \tag{1}$$

The map depends on two parameters a and b, which in the classical case have values of $a = 1.4$ and $b = 0.3$. Originally introduced as a model of a Poincaré map for a three-dimensional flow, the map displays a wide array of dynamical behaviors as its parameters are varied, [Zhiping *et al.*, 1991; Piacquadio *et al.*, 2002].

In this study, we will concentrate on the dissipative, orientation-reversing case; more precisely, we will consider $a \in [0, 2]$ and $b \in [0, 0.5]$. This region contains the classical parameter values $a = 1.4$, $b = 0.3$ for which one observes the so-called Hénon attractor (see Fig. 1). In the setting we are considering, it is known [Newhouse, 1979] that when a saddle point generates a homoclinic intersection, a cascade of (periodic) sinks will occur. Furthermore, there will be nearby parameter values for which the map has infinitely many coexisting sinks. Nevertheless, coexisting sinks for the Hénon map appear to be very elusive; due to the dissipative nature of the map, the regions in parameter space for which sinks appear simultaneously are extremely small. In this work, we report some results of the numerical search for parameter values for which there exist more than two attractors.

It is known [Benedicks & Carleson, 1991] that there is a set of parameters (near $b = 0$) with positive Lebesgue measure for which the Hénon map has a strange attractor. But given a specific point (a, b) in parameter space, it is not possible to prove that the dynamics of the map generates a strange attractor. It is, however, possible to prove the existence of a (periodic) sink; this is a finite computation, and all necessary conditions are open (and thus robust). Our study shows that in many cases where there appears to be a strange attractor, the true underlying dynamics is governed by a single (or multiple) periodic sink.
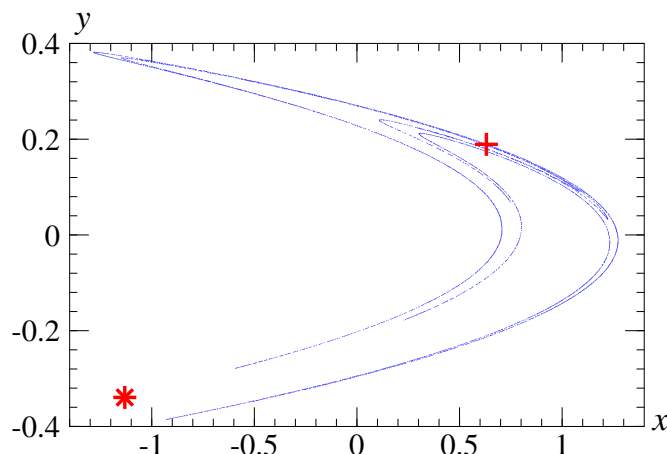
Fig. 1. Trajectory of the Hénon map (with $(a, b) = (1.4, 0.3)$) composed of 10000 points; unstable fixed points (+, ✱)

2. Numerical methods

2.1. *Search for coexisting attractors*

The most natural method to find a sink is to follow a trajectory and monitor whether it converges to a periodic orbit. First, initial iterates are discarded until a steady-state is observed. At this stage, we "restart" the trajectory by taking the current iterate as initial point. Next, we check if the trajectory periodically returns very close to this initial point. The number of iterations which should be skipped to reach the steady state depends on various factors like the eigenvalues of the periodic orbit (they define the strength with which the periodic orbit attracts neighboring trajectories), the size of the basin of attraction and its shape, including the size of the immediate basin. Usually the number of iterations which has to be discarded has to be chosen by trial-and-error.

With chaotic attractors the situation is more difficult, since a trajectory belonging to a chaotic attractor never exactly comes back to the initial point. We use an approach based on counting the number of bins visited by the trajectory at steady-state. First, the state space is covered by a finite number of bins. Again — as in the case of periodic orbits — some initial iterates are computed and discarded to reach the steady-state. At this stage, a trajectory of a fixed (long) length is computed, and the number of bins visited by the trajectory is calculated and recorded. This data is saved for several initial points. If, for two different initial points the numbers of bins are similar, then most likely the trajectories converge to the same attractor. Note that this method works for periodic attractors too. In this situation, however, if two trajectories converge to the same periodic orbit, then the number of bins should be the same. A more sophisticated (although slightly slower) approach is to also record the bin positions, and compare whether the trajectories visit the same bins. This method will distinguish two different periodic orbits of the same period, or two chaotic attractors — both having nonempty intersections with approximately the same number of bins.

In order to be able to locate coexisting attractors, it is necessary to use many initial conditions. Since some of the attractors may have very small basins of attraction, it is a good strategy to start the computations from many randomly chosen initial points. In this study, 2000 initial conditions for each point in parameter space were used.

2.2. *The existence of attractors*

To prove the existence of attractors we use methods from interval analysis [Moore, 1966; Neumaier, 1990]. These methods allow us to obtain rigorous results using computers. Computations in properly rounded interval arithmetic produce results which contain both machine arithmetic results and also true (infinite arithmetic precision) results. Using interval arithmetic it is possible, for example, to prove in a finite number of steps that an image of a given set is enclosed in other set.

Let us assume that in simulations a periodic or chaotic attractor is observed. In this section we describe a general technique to prove that there is an attractor in a neighborhood of the observed trajectory.

In order to prove that there is an attractor for the system, it is sufficient to prove that there is a positively

invariant set (a trapping region) enclosing the observed attractor. A set A is called *positively invariant* for the map f if $f(x) \in A$ for all $x \in A$. This can be established by constructing a candidate for a trapping region enclosing the region of interest, covering it by a set of interval vectors, and verifying rigorously that the image of each interval vector is enclosed by the set A. Usually one uses a covering by so called ε–boxes, i.e., interval vectors with corners lying on a rectangular grid [Galias, 2001]. Each ε–box is a an interval vector of the form $\mathbf{v} = ([k_1\varepsilon_1, (k_1 + 1)\varepsilon_1], [k_2\varepsilon_2, (k_2 + 1)\varepsilon_2], \ldots, [k_m\varepsilon_m, (k_m + 1)\varepsilon_m])$, where m is the dimension of the state space, k_i are integer numbers, and $\varepsilon = (\varepsilon_1, \varepsilon_2, \ldots, \varepsilon_m)$. This type of representation is very well suited for rigorous computations. First, by changing ε, it is possible to represent a given set by ε–boxes with arbitrary precision. Second, when ε is fixed, an ε–box is defined uniquely by m integer numbers.

In this work, we use another method. It has the advantage that no candidate set has to be defined a priori, and the trapping region is constructed by the procedure. In this method one starts with a single ε–box enclosing an arbitrary point from the observed trajectory or a covering of the numerically observed attractor by ε–boxes. This defines the set S of boxes. In each step, for each box from S its image under f is computed, and a set of ε–boxes containing the image are found. New boxes are added to the set S. The procedure is continued until no new boxes appear in the process. On the exit, the set S is a trapping region for the map f.

To prove that there is at least n attractors for the system it is sufficient to prove that there are n trapping regions, and that the trapping regions are pairwise disjoint. This is particularly easy if the trapping regions are represented as sets of ε–boxes of the same size.

It is very important to choose ε in a correct way. If ε is too large, then either we will not be able to finish the search procedure or the resulting trapping regions for different attractors will overlap. If ε is too small, then the computations will generate a covering consisting of prohibitively many boxes.

2.3. *The existence of periodic orbits*

In the previous section, we have described a general technique to prove the existence of an attractor. It involves finding images of many ε–boxes, and even for simple attractors the number of boxes which has to be used may be very large. When the attractor is periodic, one may use a faster technique.

Interval methods provide simple computational tests for uniqueness, existence, and nonexistence of zeros of a map within a given interval vector. Let $F \colon \mathbb{R}^n \mapsto \mathbb{R}^n$ be a continuous map. In order to investigate the existence of zeros of F in the interval vector $\mathbf{v}$ one evaluates a certain interval operator over $\mathbf{v}$. In this work, we use the Newton operator [Neumaier, 1990]:

$$N(\mathbf{v}) = \hat{v} - F'(\mathbf{v})^{-1}F(\hat{v}), \tag{2}$$

where $F'(\mathbf{v})$ is an interval matrix containing the Jacobian matrices $F'(v)$ for all $v \in \mathbf{v}$, and $\hat{v} \in \mathbf{v}$. In our implementation, we choose $\hat{v}$ to be the center of $\mathbf{v}$.

The most important property of the Newton operator can be used to prove the existence and uniqueness of zeros. It states that if $N(\mathbf{v}) \subset \mathbf{v}$, then F has exactly one zero in $\mathbf{v}$. Note that all operations in (2), including evaluation of $F(\hat{v})$ and $F'(\mathbf{v})$, have to be implemented rigorously in interval arithmetic for this property to be valid.

In order to study the existence of period–p orbits of a map h, we construct the map F defined by

$$[F(v)]_k = z_{(k+1) \bmod p} - h(z_k), \quad \text{for} \quad 0 \le k < p, \tag{3}$$

where $v = (z_0, z_1, \ldots, z_{p-1})$. Zeros of F correspond to period–p points of h, i.e., $F(v) = 0$ if and only if $h^p(z_0) = z_0$. In order to prove that there is a single period-p orbit enclosed in the interval vector $\mathbf{v}$ it is sufficient to evaluate the interval Newton operator on $\mathbf{v}$, and verify that $N(\mathbf{v}) \subset \mathbf{v}$. This approach combined with the generalized bisection technique has been successfully used to find all low period cycles for the Hénon map and the Ikeda map [Galias, 2001]. Application to continuous systems was presented in [Galias, 2006] and [Galias & Tucker, 2011].

Another choice is to apply the interval operator to the map $f = \mathrm{id} - h^p$. This approach involves the computation of several iterates of the map, and may — especially for longer orbits — lead to huge overestimations. The former method has an advantage that the problem of the existence of periodic orbits is translated into the problem of the existence of zeros of a higher-dimensional function. This helps to reduce the overestimation caused by the wrapping effect inherent in all set-valued computations. For details see [Galias, 2001].

Note that the Newton operator enables us to prove the existence of unstable periodic orbits as well. To show that the periodic orbit is an attractor we must show that it is asymptotically stable. This problem is handled in the following section.

2.4. *Properties of periodic orbits*

In this study, the most important property of a periodic orbit is its stability. To study the stability of the orbit $v = (z_0, z_1, \ldots, z_{p-1})$ it is sufficient to compute the Jacobian matrix J along the orbit

$$J = (h^p)'(z_0) = h'(z_{p-1}) \cdots h'(z_1) \cdot h'(z_0), \tag{4}$$

and find its eigenvalues. If both eigenvalues are within the unit circle, then the orbit is asymptotically stable. Sometimes, especially when eigenvalues are close to the unit circle, it may be easier to use the Jury criterion, which states that the second-order polynomial $\lambda^2 + a_1\lambda + a_0$ has all zeros within the unit circle if and only if $a_0 < 1$, $a_0 + a_1 + 1 > 0$, and $a_0 - a_1 + 1 > 0$.

Another important question concerning periodic orbits is the minimum period. Even if the map (3) is shown to have a single zero in a given interval vector, it does not follow that the minimum period of the corresponding periodic orbit of h is p. To be sure that p is the minimum period it is sufficient to verify that the minimum distance

$$d_{\text{self}}(v) = \min_{k \neq l} \|z_k - z_l\|_2 \tag{5}$$

between points belonging to the periodic orbit $v = (z_0, z_1, \ldots, z_{p-1})$ is positive. If the interval vectors $\mathbf{z}_0, \mathbf{z}_1, \ldots, \mathbf{z}_{p-1}$ contain points belonging to the periodic orbit it is sufficient to verify that the interval $\bigcup_{k \neq l} \|\mathbf{z}_k - \mathbf{z}_l\|_2$ does not contain 0.

2.5. *Distance between attractors*

Another problem is to verify that two attractors are different. This can be solved by computing the distance between them. The distance between two sets A and B is defined as

$$d(A, B) = \max\{\sup_{z \in A} \inf_{w \in B} \|z - w\|_2, \sup_{w \in B} \inf_{z \in A} \|z - w\|_2\}. \tag{6}$$

Two sets are different if their distance is positive. However, note that usually we do not know the exact positions of attractors; we only have the regions enclosing them. From the fact that the distance between enclosures of attractors is positive it does not follow that the attractors are different. Therefore, in general, we have to verify that the enclosures are not overlapping or, in other words, we have to compute the *infimum distance* between the two sets, which is defined as

$$d_{\text{inf}}(A, B) = \inf_{z \in A, w \in B} \|z - w\|_2, \tag{7}$$

and verify that it is positive. Formally, to show that the attractors are different, we use the following property: If sets of boxes $\bigcup_k \mathbf{z}_k$ and $\bigcup_l \mathbf{w}_l$ are enclosures of attractors A and B, respectively, and the interval $\bigcup_{k,l} \|\mathbf{z}_k - \mathbf{w}_l\|_2$ does not contain zero, then the attractors are different. The infimum distance between two attractors is also interesting from the dynamical point of view. It tells us how close two trajectories belonging to different attractors could be.

Sometimes, the enclosures of some attractors are composed of several components, and we know that the attractors have non-empty intersection with each component; this is usually the case for periodic attractors. Then, by computing distances between components we can obtain a lower bound of the distance between the attractors.

2.6. *The continuation method to find the existence region of a sink*

When a point in the parameter space with a sink is found one may use the continuation method to find a connected region in the parameter space for which this periodic orbit exists. The search is based on the assumption that the position of the orbit changes continuously with the parameters.

Usually, the most effective method to find the region of existence is to continue along the border of the region using for example the simplex continuation method [Allgower & Georg, 1980]. Unfortunately, in our case this procedure did not produce correct results: some parts of the existence regions were not found (for example one

branch of the swallowtail structure shown in the next section was missing). This failure was caused by the fact that in some cases two sinks with the same period coexist, and continuation along the border fails at points where the second sink emerges.

Therefore, we use the following method: the parameter space is covered by a rectangular grid of points, and continuation in all directions is carried out. For each grid point, sinks which were obtained by the continuation procedure in previous steps are remembered, and continuation is performed in each direction for each sink.

2.7. *Numerical study of basins of attraction*

When we detect more than one attractor for the system, an interesting challenge is to determine which trajectories converge to which attractor. For an attractor A we define its basin of attraction $B(A)$ with respect to the map f as the set of points for which a trajectory starting in this set converges to A:

$$B(A) = \{x\colon \ d(f^n(x), A) \to 0 \text{ for } n \to \infty\}. \tag{8}$$

Basins of attraction can be studied numerically by computing trajectories emanating from different initial conditions, and checking which attractor each trajectory converges to. The initial points can be selected arbitrarily, but a natural choice is to select them from a rectangular grid. To visualize the basins of attraction the positions of initial points whose trajectories tend to different attractors are plotted using different colors.

An important notion in the context of basins of attraction is the so-called immediate basin size. It is defined as the largest number r_ε such that all trajectories starting closer than r_ε from the attractor do not escape further than ε from the attractor, and converge to the attractor:

$$r_\varepsilon(A) = \arg \max_{r} \{d(f^n(x), A) \le \varepsilon \ \forall n \ge 0 \text{ and } \ d(f^n(x), A) \xrightarrow{n \to \infty} 0 \text{ for all } x \text{ such that } \ d(x, A) \le r\}. \tag{9}$$

The choice of ε is somewhat arbitrary. Usually, choosing ε a couple of times larger than the expected immediate basin size works well.

3. Results

In order to locate multiple attractors, we have performed the following search in parameter space. 1001×1001 points were chosen in the rectangle $(a, b) \in [0, 2] \times [0, 0.5]$. For each point in parameter space, 2000 initial points in phase space were randomly selected. For each such initial point, a trajectory of length 110000 was computed. The first 100000 iterations were discarded (to avoid transient behaviour), and the final 10000 iterations were used to fill bins. For binning only the x-variable was used. Divergent trajectories were detected and discarded. All initial points with less than 20% bins non-empty were recorded. Similar computations have been done for 1001×1001 points in the rectangle of parameter values $(a, b) \in [1.3, 1.5] \times [0.2, 0.4]$.

The results of these computation are reported in Table 1, where some examples of parameters for which three attractors were found are given, along with short descriptions of observed attractors. In all cases, we have proved the existence of three attractors, with the exception of case 14, where we were unable to prove the existence of the third attractor due to its very small immediate basin of attraction (further explanations are given later). In all cases where we report a sink, we have proved the existence of a sink using the interval Newton method, with the exception of the period-72 orbit for case 5. In this case the existence of the orbit was proved, but we could not verify from the Jacobian matrix that the orbit is stable. Nevertheless, the existence of an attractor enclosing this particular orbit was established using the general method described in Section 2.2.

In what follows, several examples are discussed in more details.

3.1. *The case a = 1.338, b = 0.3105*

Using the interval Newton operator, we prove that for $a = 1.338$, $b = 0.3105$ there exist three stable periodic orbits with periods 7, 15, and 30, respectively. The properties of the sinks are collected in Table 2. For each sink we report its period p, rigorous bounds of its self distance d_{self} as defined in (5), rigorous bounds for the eigenvalue λ_1 with the largest absolute value, the largest Lyapunov exponent l_1 computed as $l_1 = p^{-1} \log |\lambda_1|$ (l_1 is computed non-rigorously), the immediate basin size r_ε, and the percentage p_{conv} of trajectories converging to this sink, when finding basins of attraction.

Table 1.   Parameter values with multiple attractors

	a	b	attractors
1	1.338	0.3105	period-7, period-15, period-30
2	1.3562	0.2586	period-7, period-18, period-36
3	1.3566	0.2588	period-7, period-18, period-36
4	1.356	0.2586	period-7, period-18, period-18
5	1.3328	0.2812	period-22, period-22, period-72
6	0.98	0.4415	period-8, period-12, period-20
7	0.95	0.4795	period-8, period-14, period-16
8	0.954	0.474	period-8, period-16, period-28
9	1.4776	0.252	period-6, period-8, chaotic?
10	1.4772	0.2522	period-6, period-8, chaotic?
11	1.3568	0.2588	period-14, period-36, chaotic?
12	0.972	0.4575	period-12, period-16, chaotic?
13	0.984	0.433	period-8, period-12, chaotic?
14	1.044	0.443	period-14, period-32, chaotic?
15	0.97	0.466	period-8, chaotic?, chaotic?

Table 2. $a = 1.338$, $b = 0.3105$; properties of the sinks, p — period of the sink, d_{self} — the self distance of the sink, λ_1 — rigorous bounds for the eigenvalue with the largest absolute value, l_1 — the largest Lyapunov exponent, r_ε — the immediate basin size, p_{conv} — the percentage of trajectories converging to the sink

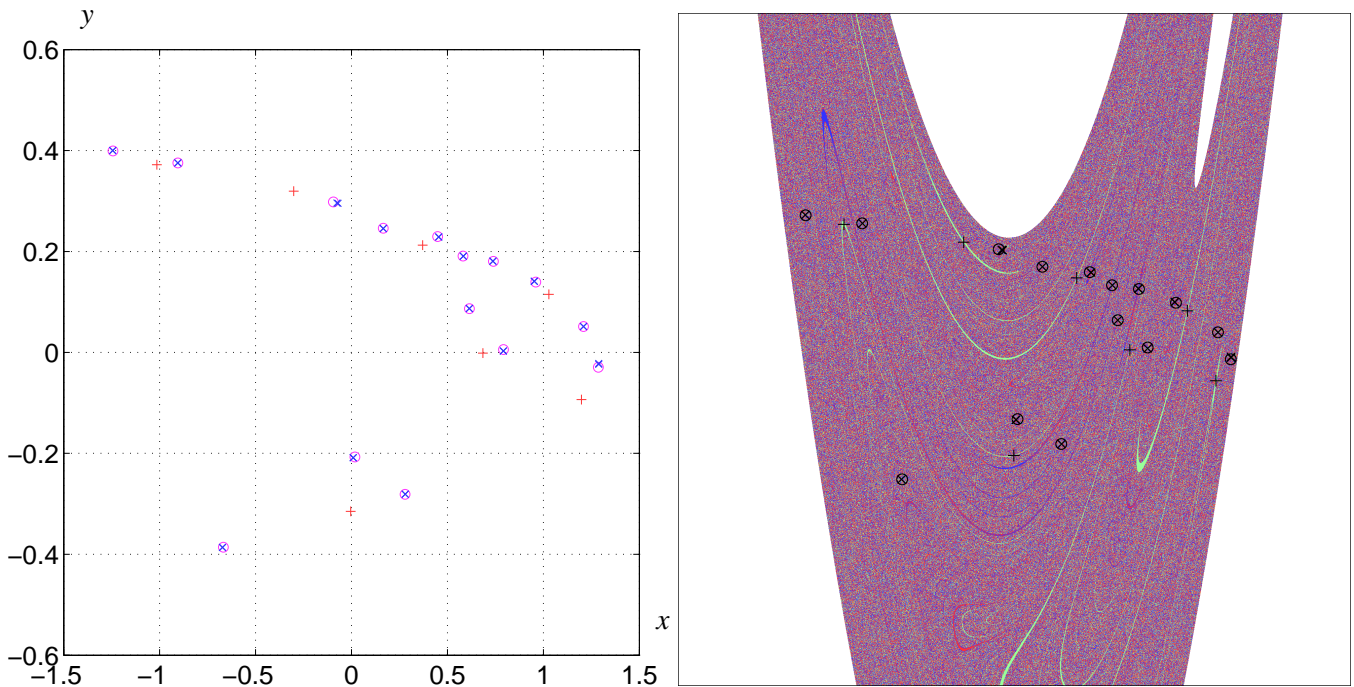| k	p	d_{self}	λ_1	l_1	r_ε	p_{conv}
1	7	$0.2686736527274^{91}_{82}$	-0.5307318760^{8}_{6}	-0.09050	$6.12 \cdot 10^{-4}$	15.12%
2	15	0.1096877106652^{7}_{5}	0.2561252^{8}_{5}	-0.09081	$4.76 \cdot 10^{-5}$	22.36%
3	30	$4.00813784^{95}_{11} \cdot 10^{-5}$	0.4208^{72}_{60}	-0.02885	$9.88 \cdot 10^{-5}$	18.56%

Fig. 2. $a = 1.338$, $b = 0.3105$, (a) period-7 sink (+), period-15 sink ($\bigcirc$), period-30 sink ($\times$), (b) basins of attraction of the three sinks, $x \in [-2, 2]$, $y \in [-1, 1]$

Table 3. $a = 1.338$, $b = 0.3105$, distances between sinks

k	l	$d_{\text{inf}}(o_k, o_l)$	$d(o_k, o_l)$
1	2	0.0727161993577_4	0.6669723627525_1
1	3	0.07955290642_6^8	0.671948186675_5^7
2	3	0.0002044048215_3	0.024230480328_5^8

The sinks are shown in Fig. 2(a). One can see that the period-7 sink is located far from the other two sinks, and that the two longer sinks almost coincide. A very low self distance of the third sink ($d_{\text{self}}(o_3) \approx 4 \cdot 10^{-5}$) indicates that the sink might be the result of the period-doubling bifurcation. Looking at the picture alone, it is difficult to say whether the two longer periodic orbits are different. The distances between the sinks computed using the formulas (6) and (7) are reported in Table 3. The results confirm that the shortest sink is far away from the other sinks (the orbit distance is larger than 0.66, and the infimum distance is larger than 0.07), and that the period-15 and period-30 orbits are located close to each other (their distance is approximately 0.024 and their infimum distance is close to 0.0002). It is clear that the sum of immediate basin sizes of two sinks has to be smaller than the infimum distance between the sinks ($4.76 \cdot 10^{-5} + 9.88 \cdot 10^{-5} < 0.000204$).

Basins of attraction of the three sinks were found numerically. 2001×2001 initial points are selected uniformly in the box $(x, y) \in [-2, 2] \times [-1, 1]$. The results are shown in Fig. 2(b). Initial points for which trajectories converge to different sinks are plotted using different colors. Initial points with diverging trajectories are left white. Thin structures corresponding to immediate basins of attraction are visible, however in most regions in the state space the basins look random. 15.12%, 22.36%, and 18.56% of trajectories converge to the period-7, period-15, and period-30 sinks, respectively. The remaining 43.96% of trajectories diverge.

Using the continuation procedure, we found regions in the parameter plane for which the three sinks observed for $a = 1.338$, $b = 0.3105$ exist. The results are shown in Fig. 3(a,b,c). In all cases the regions have a swallowtail structure (compare [Hansen & Cvitanović, 1998]). The intersection of the existence regions is shown in Fig. 3(d). This also illustrates that the existence region of the period-7 orbit is the largest, and encloses the intersection of the two other regions. A more detailed picture is shown in Fig. 3(e). In order to explain creation of the region with 3 sinks, let us denote swallowtails corresponding to period-7, period-15 and period-30 sinks by letters α, β, and γ, respectively. The branches in the swallowtail structures are numbered in the clockwise manner, in such a way that the outer branches have numbers 1 and 4 (compare Fig. 3).

One can see that some of the branches of the period-15 and period-30 swallowtails have common edges. Namely, β_3 has a common edge with γ_4 and β_1 has a common edge with γ_1. At these boundaries, the period-15 orbit looses stability, and the period-30 orbit is created via the period-doubling bifurcation. For us, it is important that β_3 — one of the inner branches of the period-15 swallowtail — has a common edge with γ_4. As a consequence, β_2 — the second inner branch of the period-15 swallowtail — intersects the γ_4 branch. The intersection has a parallelogram shape. In this region of intersection there exist three sinks — the third one is the period-7 sink, which exists in the region enclosing the whole picture (compare Fig. 3(e)).

Summarizing, the explanation of the coexistence of three sinks with different periods is the following: a part of the swallowtail structure (of the period-15 sink in the case observed) is enclosed in the region of existence of another sink (the period-7 sink in this example). Within a certain region in the swallowtail structure, two sinks with the same period (period-15 in this example) coexist. When this region is left into one of the swallowtail inner branches, one of the sinks looses stability and a stable periodic orbit is born through the period-doubling bifurcation (a period-30 orbit in the case observed).

In a neighborhood of the swallowtail, there are many other regions (perhaps infinitely many) where three sinks of various periods exist. Several examples of points belonging to these regions are plotted in Fig. 3(e) and collected in Table 4.

First, note that in a part of the swallowtail structure two sinks with the same period coexist. An example is a point $(a, b) = (1.388, 0.31046)$ plotted with the "+" symbol in Fig. 3(e). Second, note that there is a symmetric period-30 region located on the other side of the period-15 swallowtail. This region intersects the β_3 branch of the period-15 swallowtail, and as a consequence a symmetric parallelogram shaped region with three sinks of period 7, 15, and 30 exists. For example, the point $(a, b) = (1.33802, 0.31048)$ (plotted using the "$\diamond$" symbol) belongs to this
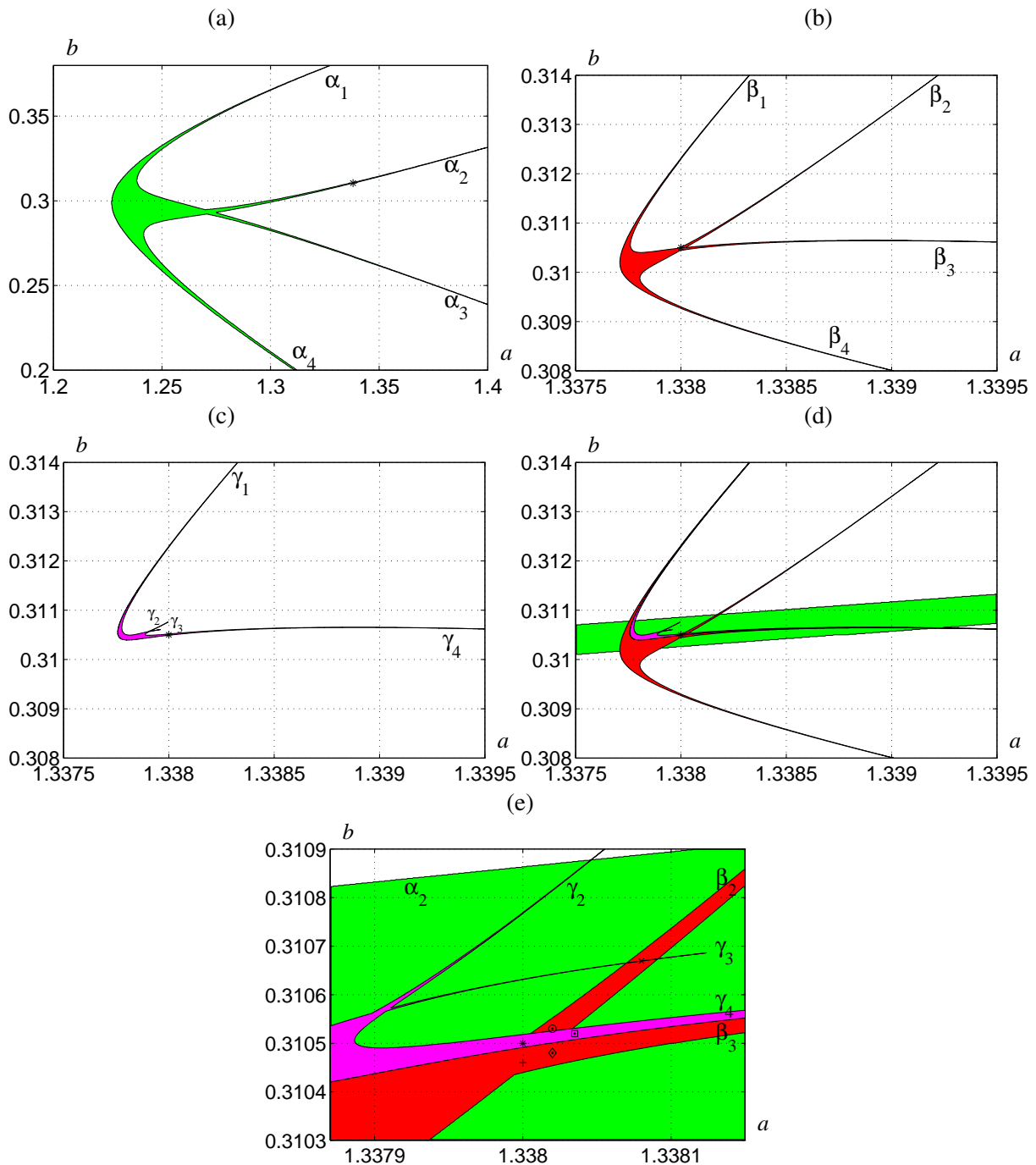
Fig. 3.   Existence regions of the three sinks, (a) period-7 sink, (b) period-15 sink, (c) period-30 sink, (d) intersection of the existence regions, (e) enlargement of (d) and positions of points belonging to other regions of coexistence of three sinks

region.

Another region is created at the intersection of two period-30 swallowtails. This happens in the corner between branches β_2 and β_3 outside the period-15 swallowtail. In the rhombus shaped region two sinks of period-30 coexist. For example, the point $(a, b) = (1.338035, 0.31053)$ (plotted with the "□" symbol) belongs to this region. Yet another region exists in the β_2 branch of the period-15 swallowtail, where a period-30 sink looses stability, and a period-60 sink is born via the period-doubling bifurcation. For example, the point $(a, b) = (1.33802, 0.31053)$ plotted with the "⊙" symbol is in this region. One may state the hypotheses that there is a sequence of period-doubling bifurcations located within the β_2 branch of the period-15 swallowtail. If this is the case, then there are infinitely many regions of coexistence of three sinks with periods 7, 15, and $15 \cdot 2^n$, for $n = 0, 1, 2, \ldots$. We have confirmed this result for

Table 4. Parameter values with multiple attractors close to $a = 1.338$, $b = 0.3105$ and a symbol used to plot the corresponding point in Fig. 3(e).

a	b	symbol	sinks periods
1.338	0.3105	✳	7, 15, 30
1.338	0.31046	+	7, 15, 15
1.33802	0.31048	◇	7, 15, 30
1.338035	0.31052	▫	7, 30, 30
1.33802	0.31053	⊙	7, 15, 60
1.33808	0.3106696	×	7, 15, 30

$n = 0, 1, 2$.

The final interesting region which we describe here is created by the intersection of the γ_3 branch of the period-30 swallowtail and the β_2 branch of the period-15 swallowtail. The point $(a, b) = (1.33808, 0.3106696)$ plotted with the "×" symbol belongs to this region. One can expect that similarly the period-60 structure intersects the period-15 swallowtail, and another region is created.

Using interval methods, we have verified that all periodic orbits listed in Table 4 exist and are stable, with the exception of the period-60 orbit, for which only the existence has been proved. Here, the Jacobian matrix obtained has very wide entries, and a rigorous computation of the eigenvalues is not feasible. Naturally, it would be possible to use higher precision interval arithmetic to prove stability in this case.

3.2. The case $a = 1.3562$, $b = 0.2586$

We prove that for $a = 1.3562$, $b = 0.2586$ there exist three sinks with periods 7, 18, and 36, respectively. Properties of the sinks are collected in Table 5.

Table 5. $a = 1.3562$, $b = 0.2586$; properties of the sinks

	p	d_{self}	λ_1	l_1	r_ε	p_{conv}
1	7	0.3089828063590^9_6	0.12690695455^9_2	-0.2949	0.000354	5.38%
2	18	0.0078666588118^4_0	-0.25477193^3_1	-0.07597	0.000734	32.46%
3	36	0.0001512680908^8_6	-0.97066^8_5	-0.000827	0.000295	18.08%

The sinks and their basins of attraction are plotted in Fig. 4. The structure of basins of attraction is similar to the previous case (compare Figure 2(b)). This time much fewer trajectories (only 5.38%) converge to the period-7 sink.

The existence regions of the period-7, period-18, and period-36 stable periodic orbits obtained using the continuation method are shown in Fig. 5. The situation is similar to the case $a = 1.338$, $b = 0.3105$. The main difference here is that the size of the period-7 region in the area of interest is much smaller. Actually, this is another branch of the period-7 swallowtail structure discussed earlier (see Fig. 3(a)). Another difference is that the swallowtail structure is less symmetric. But the explanation for the emergence of three sinks is the same. Part of the swallowtail structure of the period-18 sink is enclosed in the region of existence of the period-7 sink. One of the period-18 sinks undergoes the period-doubling bifurcation, and a period-36 sink is born. As in the previous case, other regions with three sinks in the neighborhood of the swallowtail structure can also be observed.

3.3. The case $a = 0.98$, $b = 0.4415$

Using the interval Newton operator, we establish that for $a = 0.98$, $b = 0.4415$ there exist three stable periodic orbits with periods 8, 12, and 20, respectively. Properties of the sinks are collected in Table 6.

The sinks and their basins are shown in Fig. 6(a). Note that the stripes in basin structures are much wider than in the previous examples. This is related to considerably larger immediate basin size of the period-8 sink.

The existence regions of the period-8, period-12, and period-20 stable periodic orbits obtained using the continuation method are shown in Fig. 7(a,b,c). Note that the first structure is rather complex. The intersection of the
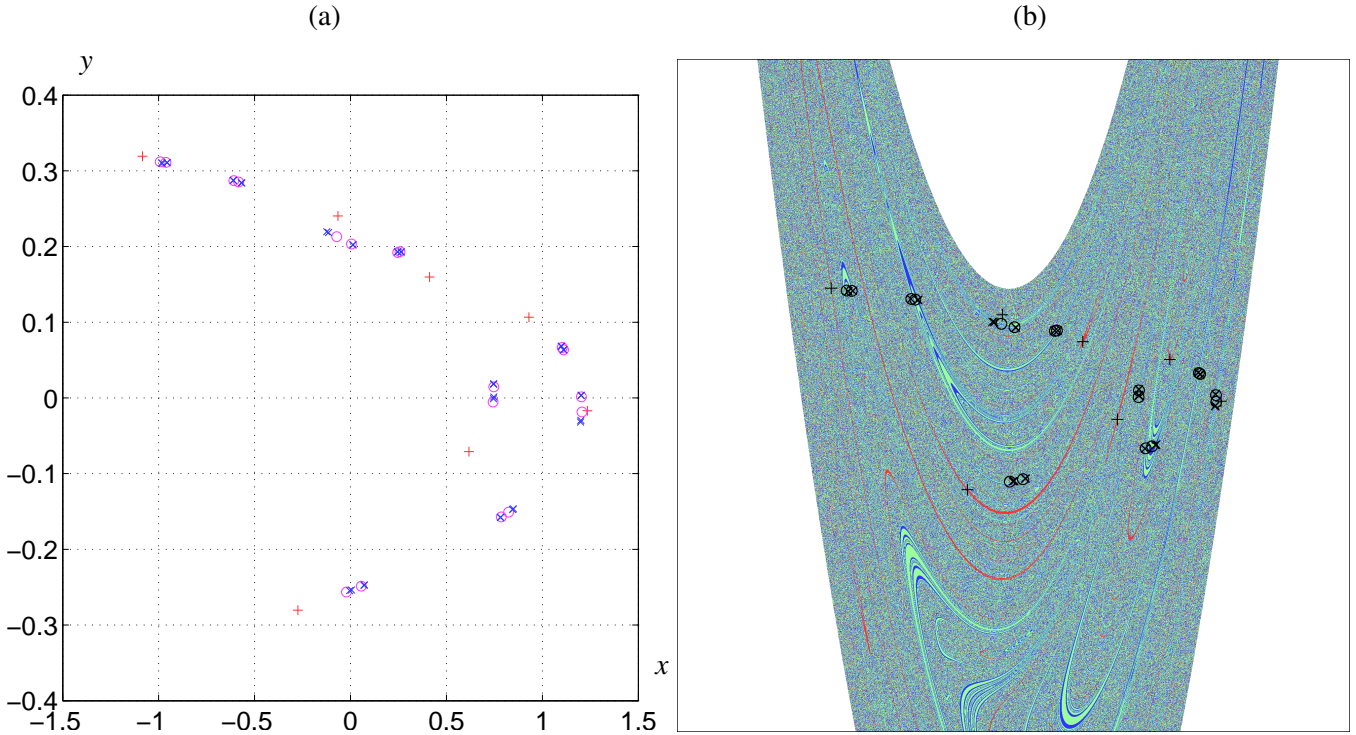
Fig. 4. $a = 1.3562$, $b = 0.2586$, (a) period-7 sink (+), period-18 sink (○), period-36 sink (×), (b) basins of attraction of the three sinks, $x \in [-2, 2]$, $y \in [-1, 1]$
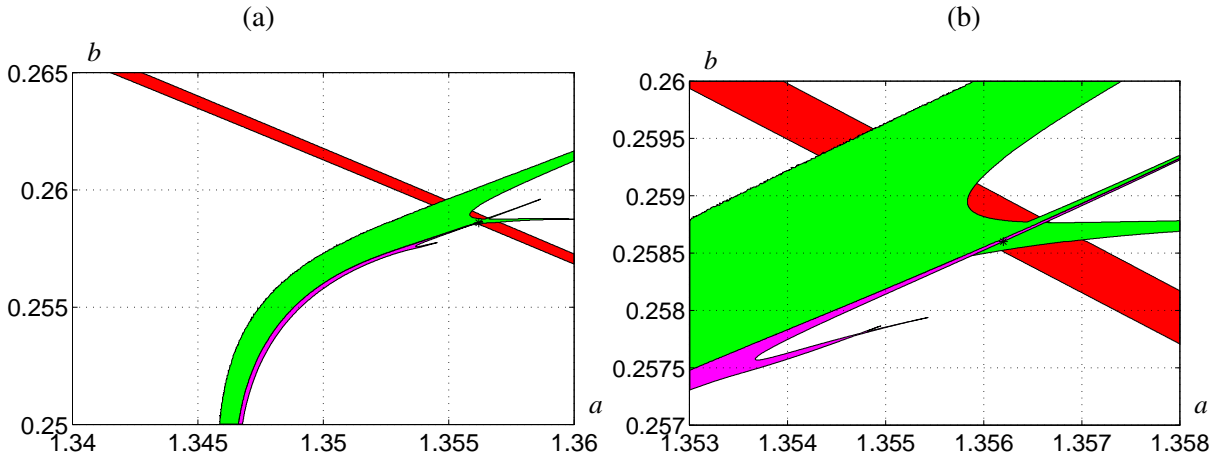

Fig. 5.   (a) Existence regions of the three sinks around $a = 1.3562$, $b = 0.2586$, (b) enlargement of (a)

Table 6. $a = 0.98$, $b = 0.4415$; properties of the sinks

	p	d_{self}	λ_1	l_1	r_ε	p_{conv}
1	8	0.309179352655_1^3	-0.892620405455_2^6	-0.01420	0.00315	5.87%
2	12	0.06905465118011_0^7	-0.437307933_4^6	-0.06892	0.00042	6.96%
3	20	0.0210560235_{67}^{70}	-0.8086767_3^7	-0.01062	0.000057	63.61%

existence regions is shown in Fig. 7(d). The regions of existence of the sinks are not related as in the previous examples. They do not have a common border and do not form a common structure like the swallowtail in the previous examples. Hence, the explanation of the coexistence of three sinks in this example is different; one may say that the sinks are "independent".
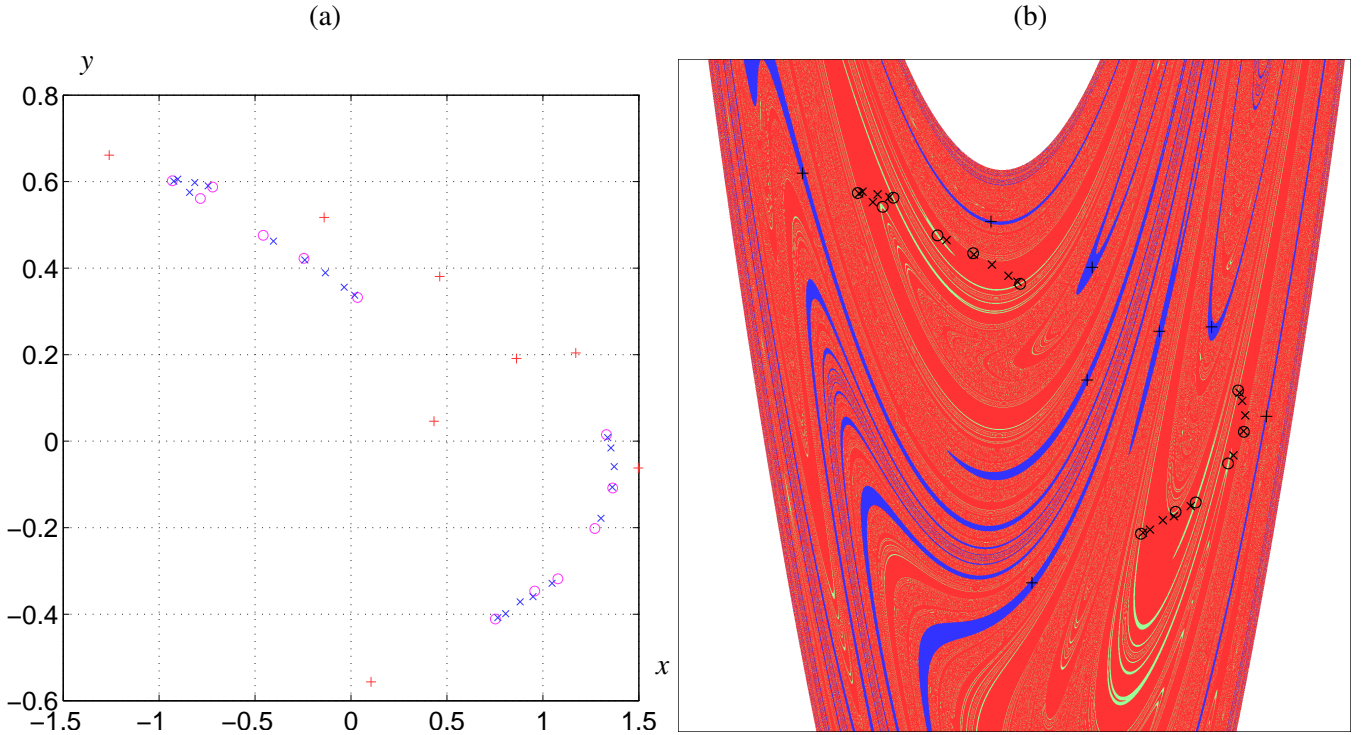
(a)

(b)

Fig. 6. $a = 0.98$, $b = 0.4415$, (a) period-8 sink (+), period-12 sink ($\circ$), period-20 sink ($\times$), (b) basins of attraction, $x \in [-2, 2]$, $y \in [-1, 1]$

Table 7. $a = 0.95$, $b = 0.4795$; properties of the sinks

	p	d_{self}	λ_1	l_1	r_ε	p_{conv}
1	8	0.3631774036692^6_3	0.77173992057_2	-0.03239	0.002191	6.24%
2	14	0.1577899141178^5_3	-0.345741481^{81}_{79}	-0.07586	0.0000988	0.69%
3	16	0.003130897223^5_3	0.9505443^6_4	-0.00317	0.003155	71.57%

Note that the intersection of the period-12 and period-20 regions is not entirely enclosed in the period-8 region. Hence, one can expect that there is another region with three sinks located within the intersection of the period-12 and period-20 regions just above the period-8 region. Indeed, we have verified that for $a = 0.97842$, $b = 0.445$ there are three sinks with periods 12, 16, and 20, respectively (compare also Fig. 7(d)). The second sink is created via the period-doubling bifurcation from the period-8 sink.

One may expect a sequence of period-doubling bifurcations and corresponding period-$(8 \cdot 2^n)$ regions. This may create a finite or infinite sequence of regions with three sinks depending on how wide the period-$(8 \cdot 2^n)$ regions are.

3.4.   *The case a = 0.95, b = 0.4795*

Using the interval Newton operator, we prove that for $a = 0.95$, $b = 0.4795$ there exist three stable periodic orbits with periods 8, 14, and 16, respectively. Properties of the sinks are collected in Table 7.

The distances between sinks are collected in Table 8. Note that the sinks are located further away from each other compared to the previous examples.

The sinks and their basins of attraction are plotted in Fig. 8. Note that only 0.69% of trajectories converge to the period-14 sink. Its immediate basin size is very small ($r_\varepsilon \approx 0.0000988$). Most orbits converge to the period-16 sink with the largest immediate basin size of $r_\varepsilon \approx 0.003155$.

The results on the existence of the sinks obtained using the continuation method are shown in Fig. 9. First, note that the region of existence of the period-8 sink is the same as the one in Fig. 7(a). The region of existence of the period-14 sink is very narrow. Finding a point belonging to this region using brute-force computations requires very fine sampling of the parameter space. Also note that the regions intersect many times and as in the previous example
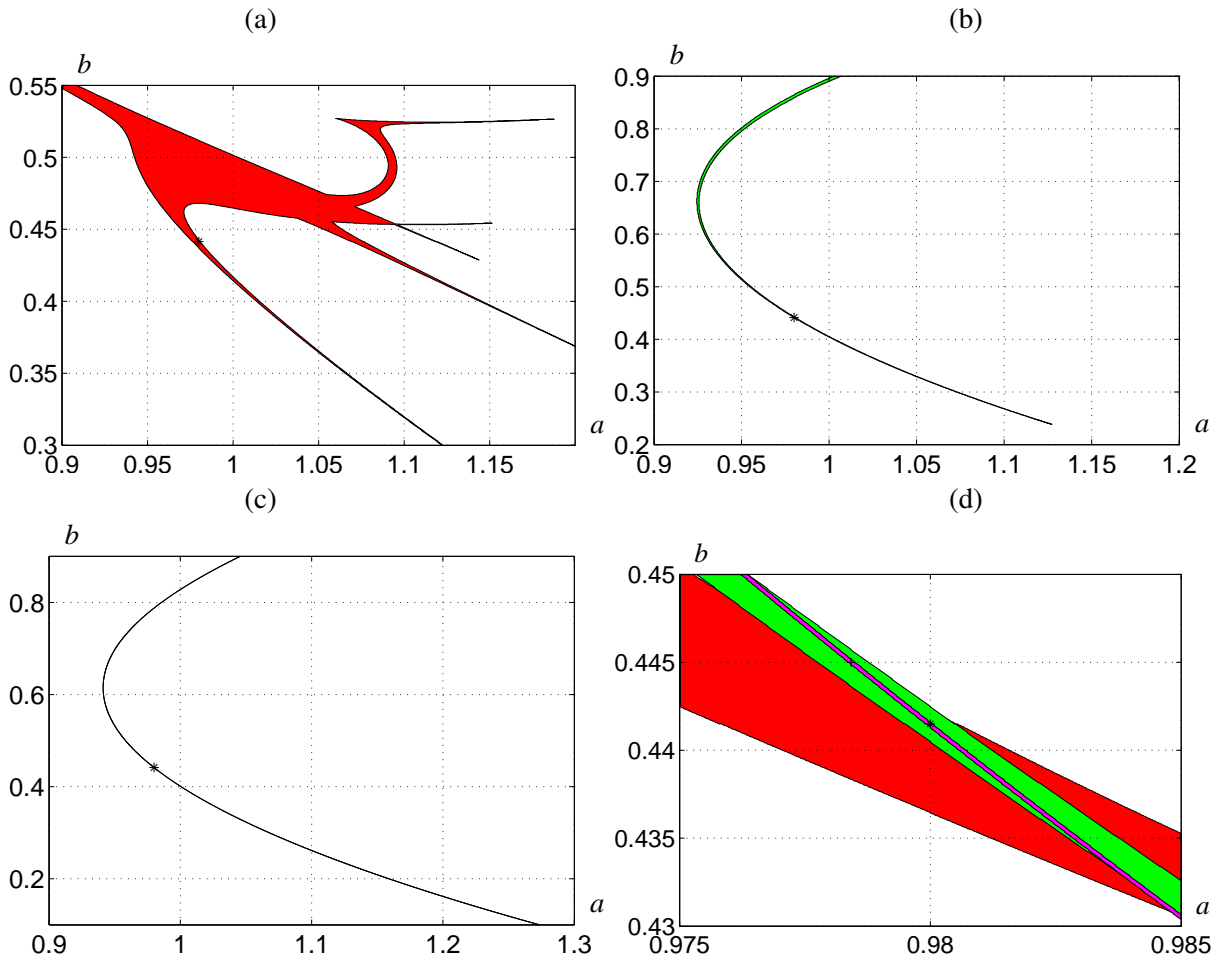
(a)

(b)

(c)

(d)

Fig. 7.   Existence regions of the three sinks around $a = 0.98$, $b = 0.4415$, (a) period-8 orbit, (b) period-12 orbit, (c) period-20 orbit, (d) borders of the existence regions at the intersection

Table 8. $a = 0.95$, $b = 0.4795$, distances between sinks

k	l	$d_{inf}(o_k, o_l)$	$d(o_k, o_l)$
1	2	0.0234358696711^8_6	0.521438589211^9_7
1	3	0.144896867601^6_2	0.859311262353^2_0
2	3	0.087504266418^6_0	0.723205660^9_7

do not have a common border.

3.5.   *The case a = 0.972, b = 0.4575*

In all previous examples, we found three coexisting sinks. For $a = 0.972$, $b = 0.4575$, however, we observe two stable periodic orbits and a third attractor which appears to be chaotic.

Using the interval Newton operator we prove that in this case there exist two stable periodic orbits with periods 12, and 16, respectively. Properties of the attractors are collected in Table 9.

The three numerically observed attractors are shown in Fig. 10. The period-16 attractor looks like a period-8 orbit; its self distance is only $d_{self} = 0.004543$. The period-12 orbit is located very close to what appears to be a chaotic attractor.

Using the technique described in Sec. 2.2, we prove that for $a = 0.972$, $b = 0.4575$ there are three non-overlapping trapping regions. For this we used ε–boxes with $\varepsilon = (2 \cdot 10^{-5}, 2 \cdot 10^{-5})$. The trapping regions found for the period-12 sink, period-16 sink and the third attractor are composed of 9527, 20425, and 320319 ε–boxes,
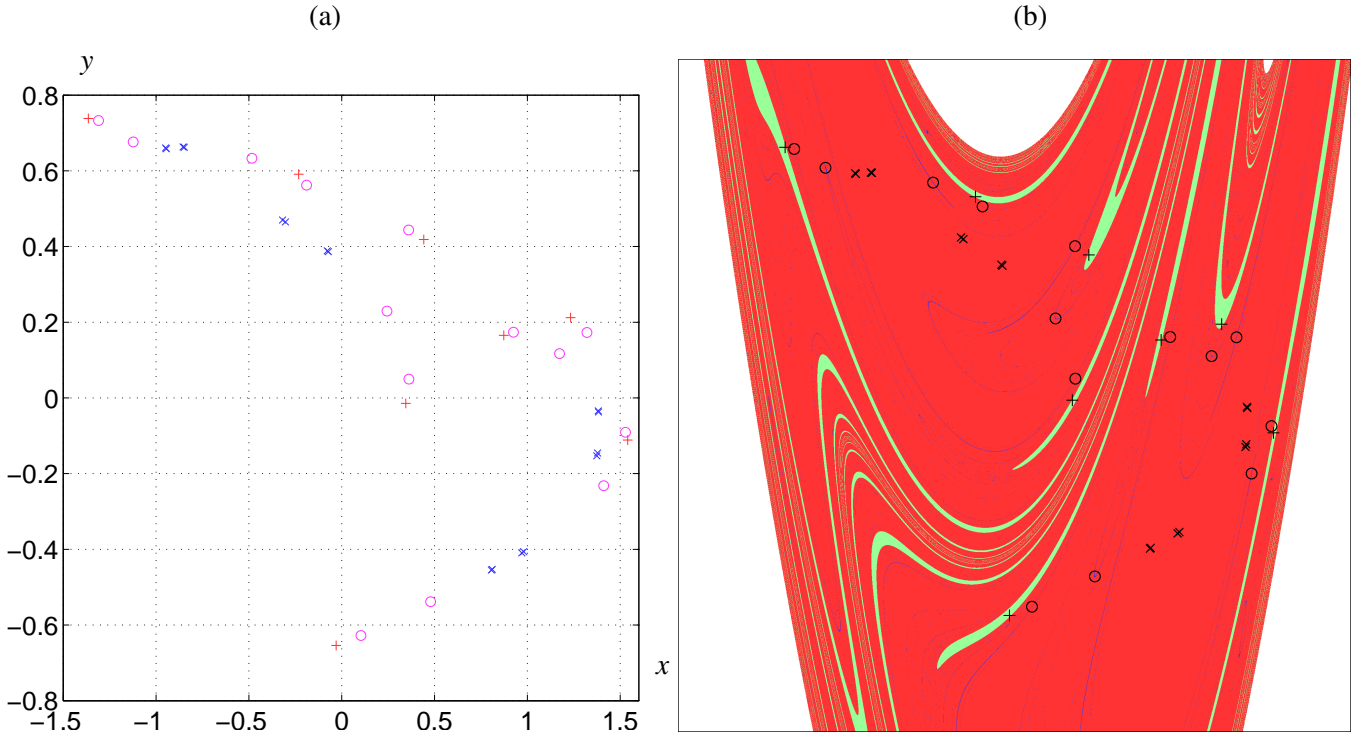
(a)

(b)

Fig. 8. $a = 0.95$, $b = 0.4795$, (a) period-8 sink (+), period-14 sink (×), period-16 sink (○), (b) basins of attraction, $x \in [-2, 2]$, $y \in [-1, 1]$

(a)

(b)
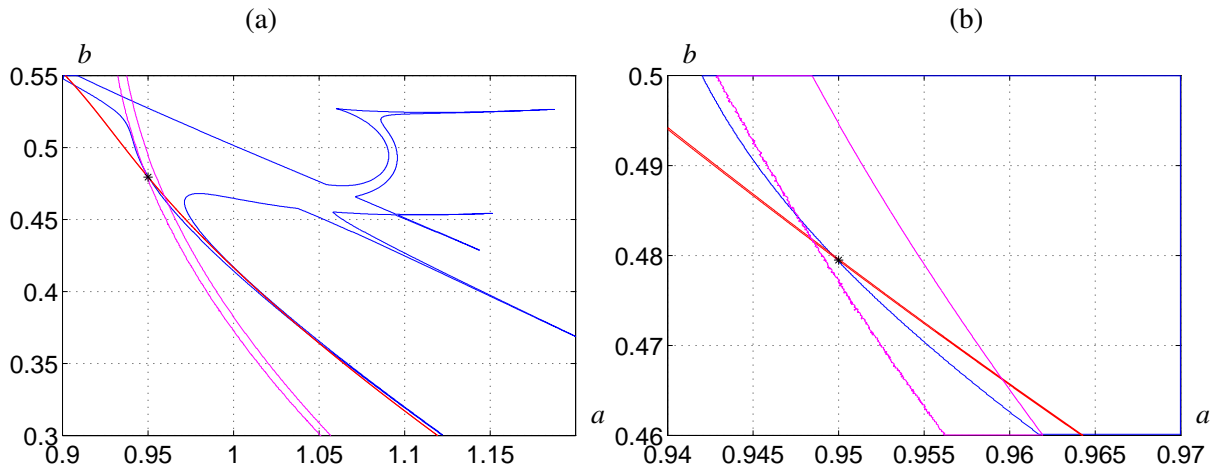

Fig. 9. (a) Existence regions of three sinks around $a = 0.95$, $b = 0.4795$, (b) enlargement of (a)

Table 9. $a = 0.972$, $b = 0.4575$; properties of the attractors

	p	d_{self}	λ_1	l_1	r_ε	p_{conv}
1	12	0.0693215779289^9_6	0.12472929^5_3	-0.1734	0.000353	5.15%
2	16	0.0028841938^6_4	0.9722667^2_0	-0.00175	0.004543	9.37%
3	∞?	0?				62.44%

respectively. The trapping region for the chaotic attractor is composed of four components. For larger boxes the method fails; when $\varepsilon = (10^{-4}, 10^{-4})$ the trapping region found for the period-12 orbit encloses both the period-12 orbit and the third attractor.
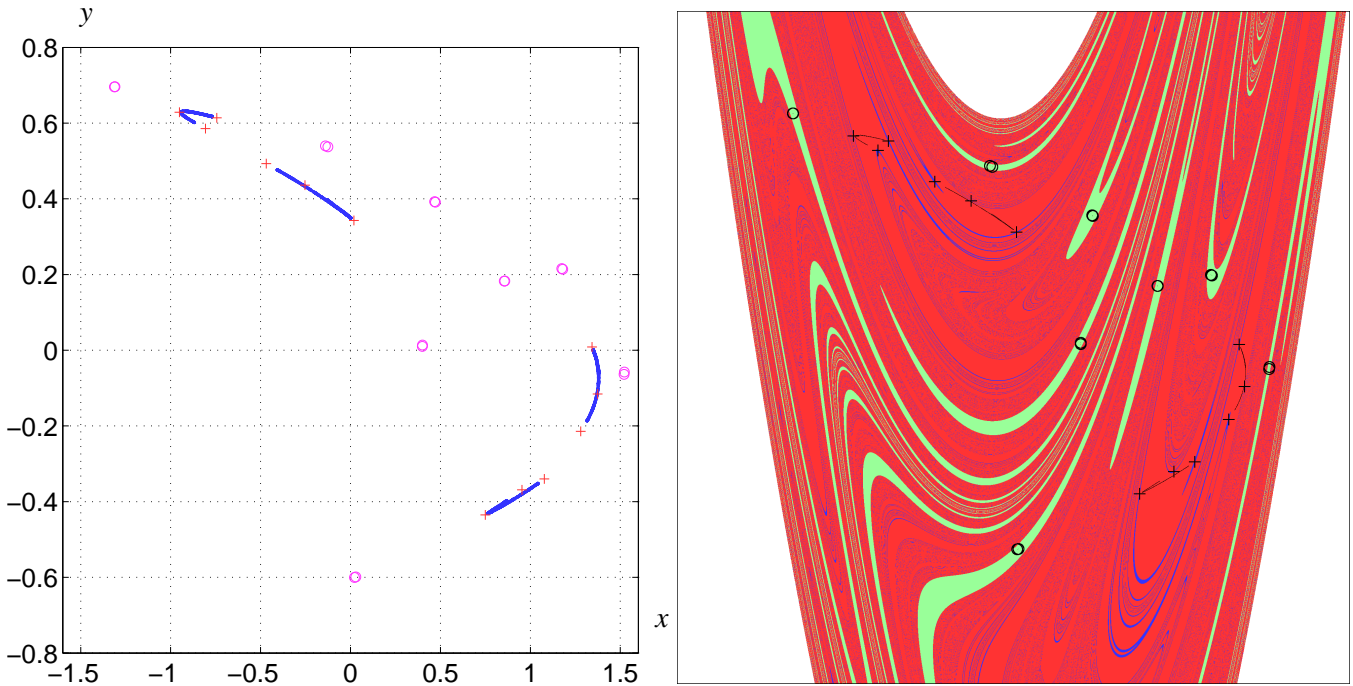
Fig. 10. $a = 0.972$, $b = 0.4575$, (a) period-12 sink (+), period-16 sink (○), and chaotic (?) attractor (dots), (b) basins of attraction, $x \in [-2, 2]$, $y \in [-1, 1]$

Table 10. $a = 0.984$, $b = 0.433$; properties of the attractors

	p	d_{self}	λ_1	l_1	r_ε	p_{conv}
1	8	0.3068270242228^6_4	-0.0913103905^8_5	-0.29918	0.002629	3.56%
2	12	0.070865817192^8_6	0.0345948^8_6	-0.28033	0.000424	6.02%
3	∞?	0?				66.60%

3.6.   *The case a = 0.984, b = 0.433*

In this case, we also observe two sinks and a (possibly) chaotic attractor. The difference is that the chaotic attractor now occupies a much smaller area in the state space. Using the interval Newton operator we show that for $a = 0.984$, $b = 0.433$ there exist two stable periodic orbits with periods 8, and 12, respectively. Properties of the attractors are collected in Table 10.

The attractors are shown in Fig. 11. Again, we can prove that there are three non-overlapping trapping regions in this case. For this ε–boxes with $\varepsilon = (2 \cdot 10^{-6}, 2 \cdot 10^{-6})$ were used. The trapping regions found for the period-8 sink, period-12 sink and the third attractor are composed of 1539, 6527, and 193161 ε–boxes, respectively. The trapping region for the chaotic attractor is composed 20 components. Therefore, one may expect that the attractor is created by a sequence of period-doubling bifurcations originating from a period-20 sink.

3.7.   *The case a = 1.044, b = 0.443*

In this case, as in two previous cases we also observe two sinks and a (possibly) chaotic attractor. This case is interesting because we were able to locate many regions with three sinks in its neighborhood.

The attractors and their basins of attraction are plotted in Fig. 12. Not that the attractors are more separated from each other than in the previous example.

Using the interval Newton operator we prove that for $a = 1.044$, $b = 0.443$ there exist two stable periodic orbits with periods 14 and 32, respectively. Properties of the attractors are collected in Table 11. For the period-32 orbit we were not able to compute the eigenvalues. Nevertheless, the orbit was proved to be stable using Jury's criterion.
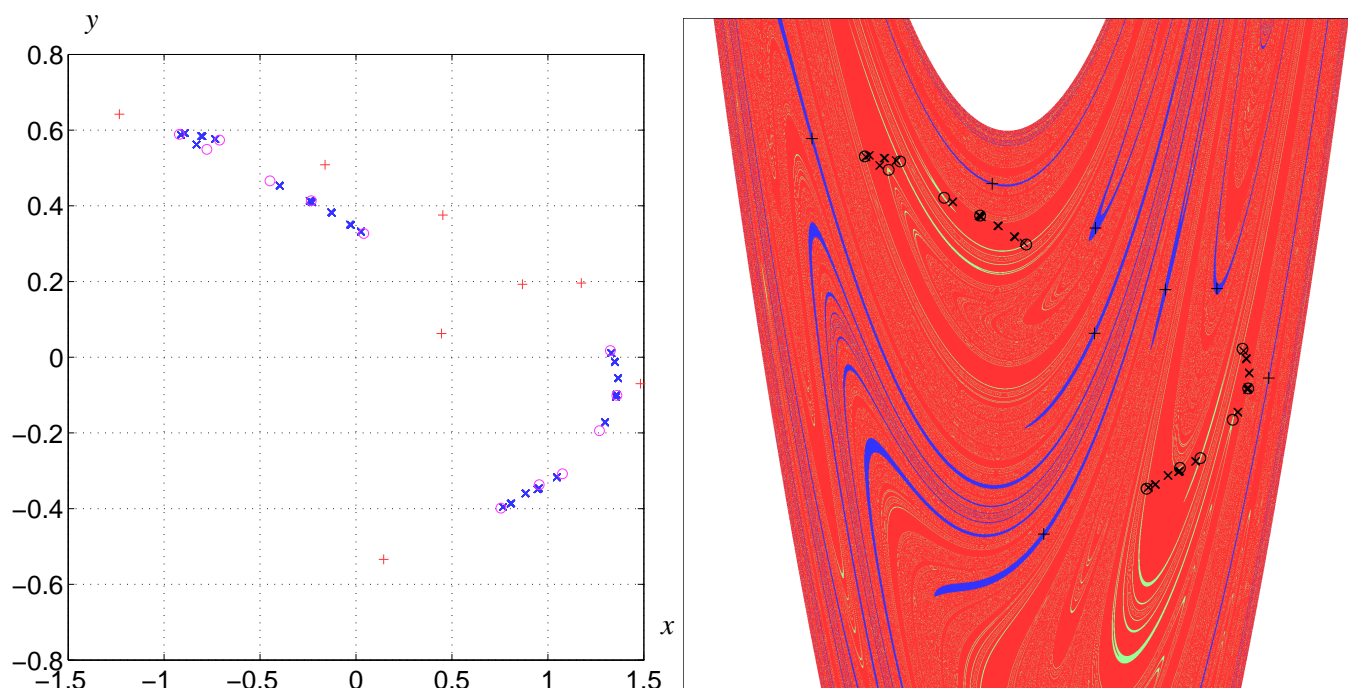
Fig. 11. $a = 0.984$, $b = 0.433$, (a) period-8 sink (+), period-12 sink (◯), and chaotic (?) attractor (×), (b) basins of attraction, $x \in [-2, 2]$, $y \in [-1, 1]$

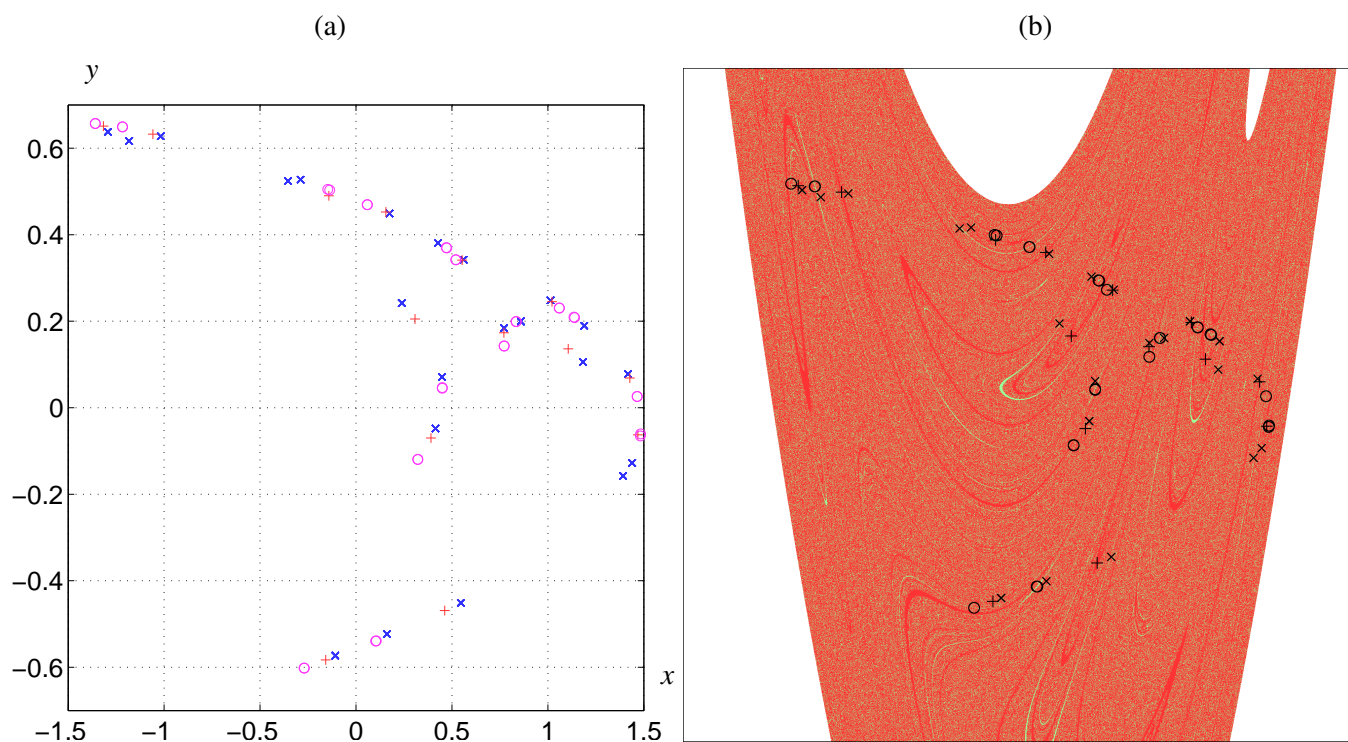(a)   (b)

Fig. 12. $a = 1.044$, $b = 0.443$, period-12 sink (◯), period-32 sink (+) and a chaotic(?) attractor (×), (b) basins of attraction, $x \in [-2, 2]$, $y \in [-1, 1]$

Despite our attempts to use various sizes of ε–boxes, we were not able to prove the existence of a trapping region enclosing the third attractor. This is perhaps due to its very small basin of attraction, only 0.52% of the computed trajectories converge to this attractor.

Table 11. $a = 1.044$, $b = 0.443$; properties of the attractors

	p	d_{self}	λ_1	l_1	r_ε	p_{conv}
1	14	0.1378260412238^5_3	-0.1766210^4_1	-0.12384	0.000354	54.08%
2	32	0.000388127246^6_4	?	-0.21467	0.000057	16.75%
3	∞?					0.52%

One can expect that the (seemingly) chaotic attractor is created by a sequence of period doubling bifurcations. If this is the case there could be a parameter region close to $a = 1.044$, $b = 0.443$ with three sinks. To confirm this hypothesis we have carried out a local search for multiple attractors. A number of points in the parameter space with three coexisting sinks were located. The results are collected in Table 12. For each region with three sinks only one example is given.

Table 12.   Parameter values with three sinks close to $a = 1.044$, $b = 0.443$

a	b	sinks periods
1.04396	0.443	14, 16, 22
1.04396	0.442999	14, 16, 44
1.043914	0.443026	14, 16, 32
1.043908	0.442985	14, 16, 42
1.043922	0.442984	14, 16, 84
1.043902	0.442999	14, 16, 88
1.04397	0.443	14, 22, 32
1.044042	0.443001	14, 22, 64
1.044038	0.442976	14, 32, 42
1.04398	0.443	14, 32, 44
1.044008	0.443	14, 32, 66
1.044066	0.442974	14, 32, 84
1.043994	0.443,	14, 32, 88
1.044096	0.442972	14, 42, 64

We have proved that for $a = 1.04396$ and $b = 0.443$ there exist three sinks with periods 14, 16, and 22, respectively. It is interesting to know that their immediate basin sizes are $2.94 \cdot 10^{-4}$, $9.88 \cdot 10^{-5}$, and $3.47 \cdot 10^{-7}$, respectively. The extremely small value of the immediate basin size for the third sink might be the reason why it was not possible to find a trapping region enclosing the chaotic attractor for $a = 1.044$, $b = 0.443$. Note that finding a trapping region for the period-22 orbit for $a = 1.04396$, $b = 0.443$ also did not work.

One can see from Table 12 that in a neighborhood of the point $a = 1.044$, $b = 0.443$ there are many different regions with three coexisting sinks. In order to get a better understanding of the relations between these regions, we have found existence regions of various sinks. The search was performed using the continuation method started at points from Table 12. The results are shown in Fig. 13. The largest region is the region of existence of period-14 sink. Apart from it there are three structures of parallel stripes. Two of them are very narrow. The widest structure contains regions of existence of seven sinks. The first three of them are period-16, period-32, and period-64 sinks. The corresponding existence regions have common borders, which means that period-32 and period-64 sinks are born by the period-doubling bifurcation. The widest structure contains also four narrow parallel stripes, which are the regions of existence of period-80, period-48, period-80 and period-64 sinks. Note that these regions are separated from each other. The second set of parallel stripes (labelled "22") is almost horizontal. Although it is very narrow (in fact one can see only a single stripe in the picture), it contains four existence regions. The regions of existence of period-22, period-44, and period-88 sinks have common borders. The last stripe in this structure is the region of existence of a period-66 sink, and is separated from other stripes in this structure. The last structure (labelled "42") contains regions of existence of period-42 and period-84 sinks.

The intersection of each of the two stripes belonging to the parallel structures described above creates a region of existence of three sinks. It follows that there are at least 50 ($7 \cdot 4 + 7 \cdot 2 + 4 \cdot 2$) distinct regions of coexistence of three sinks shown in Fig. 13. Some examples were already given in Table 12.
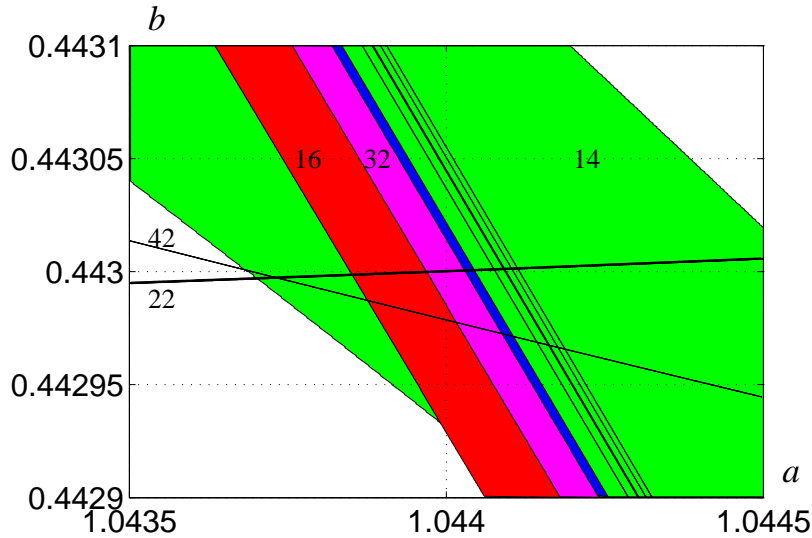
Fig. 13. Existence regions of three sinks around $a = 1.044$, $b = 0.443$

Table 13. $a = 0.97$, $b = 0.466$; properties of the attractors

	p	d_{self}	λ_1	l_1	r_ε	p_{conv}
1	8	0.3320789682392_7^9	-0.896893877753_2^8	-0.0136	0.00785	12.80%
2	∞?	0?				55.27%
3	∞?	0?				8.17%

3.8. *The case a = 0.97, b = 0.466*

In the previous three cases, two sinks and one (possibly) chaotic attractor were observed. In the present case we have only one periodic attractor, and two potentially chaotic attractors. The existence of the sink is established using the interval Newton operator. Properties of the attractors are collected in Table 13. The three attractors and their basins of attraction are shown in Fig. 14.

Using the technique described in Sec. 2.2, we prove that there are three non-overlapping trapping regions. For $\varepsilon = (10^{-4}, 10^{-4})$ the trapping regions found for the two chaotic attractors overlap. For $\varepsilon = (10^{-5}, 10^{-5})$, the three trapping regions do not overlap. They are composed of 8385, 141836, and 805095 ε–boxes, respectively. These trapping regions are composed of 8, 12, and 4 connected regions respectively. Using $\varepsilon = (2 \cdot 10^{-6}, 2 \cdot 10^{-6})$ gives trapping regions composed of 9369, 629260, and 225434 boxes. The last trapping region is decomposed into 20 connected components, which is a much finer enclosure of the attractor.

4. Conclusions

In this paper, we have explored a large parameter domain for the Hénon map, and located regions for which there are (at least) three coexisting attractors. In the strongly dissipative case ($b \in [0, 0.5]$) that we have considered, it is hard to find sinks due to their small immediate basins of attraction. The attractors were located by an ensemble of brute-force computations, and later verified by interval analysis and rigorous numerics. This ensures that the reported sinks are not numerical artifacts, but true mathematical objects. In order to understand the creation (and destruction) of coexisting sinks, we computed their local existence regions. This provided a clear picture of the local dynamics, and also suggested other parameter regions where coexisting sinks reside.

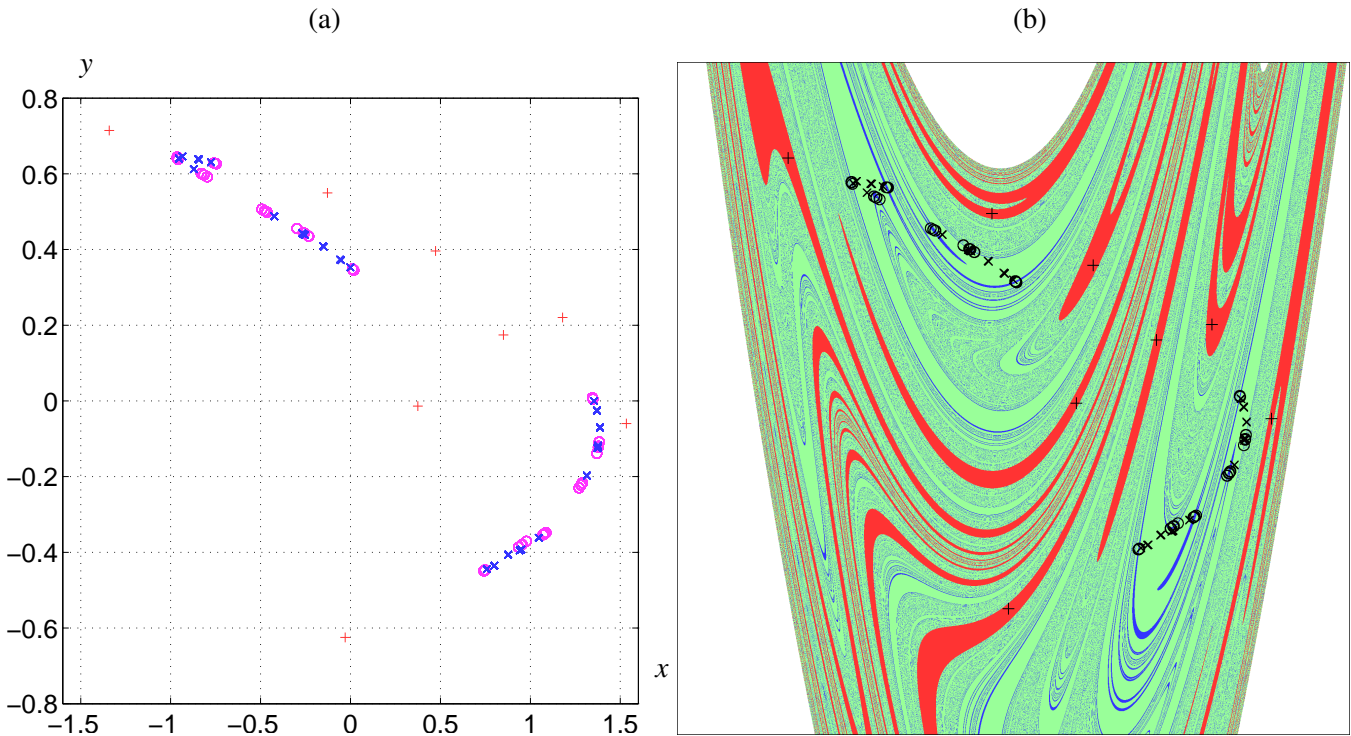## Acknowledgments

(a)   (b)

Fig. 14. $a = 0.97$, $b = 0.466$, (a) period-8 sink ($+$), first chaotic(?) attractor ($\circ$), second chaotic(?) attractor ($\times$), (b) basins of attraction, $x \in [-2, 2]$, $y \in [-1, 1]$

References

Allgower, E. & Georg, K. [1980] "Simplicial and continuation methods for approximating fixed points and solutions to systems of equations," *SIAM Review* **22**, 28–85.

Benedicks, M. & Carleson, L. [1991] "The dynamics of the Hénon map," *Annals of Mathematics* **133**, 73–169.

Galias, Z. [2001] "Interval methods for rigorous investigations of periodic orbits," *Int. J. Bifurcation and Chaos* **11**, 2427–2450.

Galias, Z. [2006] "Counting low-period cycles for flows," *Int. J. Bifurcation and Chaos* **16**, 2873–2886.

Galias, Z. & Tucker, W. [2011] "Validated study of the existence of short cycles for chaotic systems using symbolic dynamics and interval tools," *Int. J. Bifurcation and Chaos* **21**, 551–563.

Hansen, K. & Cvitanović, P. [1998] "Bifurcation structures in maps of Hénon type," *Nonlinearity* **11**, 1233–1261.

Hénon, M. [1976] "A two dimensional map with a strange attractor," *Commun. Math. Phys.* **50**, 69–77.

Moore, R. [1966] *Interval Analysis* (Prentice Hall, Englewood Cliffs, NJ).

Neumaier, A. [1990] *Interval methods for systems of equations* (Cambridge University Press).

Newhouse, S. [1979] "The abundance of wild hyperbolic sets," *Publ. Math. Inst. Hautes Etudes Sei.* **50**, 101–151.

Piacquadio, M., Hansen, R. & Ponta, F. [2002] "On the Mendès France fractal dimension of strange attractors: the Hénon case," *Int. J. Bifurcation and Chaos* **12**, 1549–1563.

Zhiping, Y., Kostelich, E. & Yorke, J. [1991] "Calculating stable and unstable manifolds," *Int. J. Bifurcation and Chaos* **1**, 605–623.